Finite Element Modeling of Shape Changes in Plant Cells[1][OPEN]

Amir J. Bidhendi[a] and Anja Geitmann[a,b,2]

[a]Institut de recherche en biologie végétale, Département de sciences siologiques, Université de Montréal, Montreal, Quebec, Canada H1X 2B2

[b]Department of Plant Science, McGill University, Macdonald Campus, Ste-Anne-de-Bellevue, Quebec, Canada H9X 3V9

ORCID IDs: 0000-0002-7482-7444 (A.J.B.); 0000-0003-0390-0517 (A.G.).

Plant cells come in a striking variety of different shapes. Shape formation in plant cells is controlled through modulation of the cell wall polymers and propelled by the turgor pressure. Understanding the shaping aspects of plant cells requires knowledge of the molecular players and the biophysical conditions under which they operate. Mechanical modeling has emerged as a useful tool to correlate cell wall structure, composition, and mechanics with cell and organ shape. The finite element method is a powerful numerical approach employed to solve problems in continuum mechanics. This Update critically analyzes studies that have used finite element analysis for the mechanical modeling of plant cells. Focus is on models involving single cell morphogenesis or motion. Model design, validation, and predictive power are analyzed in detail to open future avenues in the field.

The cell wall, a polysaccharide-rich extracellular matrix, gives plant cells their shape at the expense of constraining their growth and movement. All cellular growth processes and shape changes involve a deformation of this extracellular matrix and are controlled by it. This control is exerted by modulating the mechanical properties of the matrix, which, in turn, are regulated by the polymers present in the wall and the state of linkages between them. The main polysaccharides of the primary cell wall are pectins, cellulose microfibrils, and xyloglucans (Bidhendi and Geitmann, 2016; Cosgrove, 2016). Cellulose microfibrils are recognized as the primary load-bearing component limiting cellular expansion (Baskin, 2005; Geitmann and Ortega, 2009). However, an increasing amount of evidence points at pivotal functions of pectins and hemicelluloses in defining the mechanics of the cell wall (Parre and Geitmann, 2005; Peaucelle et al., 2011; Palin and Geitmann, 2012; Braybrook and Peaucelle, 2013;

Amsbury et al., 2016; Bidhendi and Geitmann, 2016; Torode et al., 2017). To understand how modulation of the plant cell wall affects and regulates the change of cell shape, the biomechanical context must be considered; for instance, see the Update in this issue on wall structure, mechanics, and growth (Cosgrove, 2018) or previous reviews (Geitmann and Ortega, 2009; Bidhendi and Geitmann, 2016).

Biological experimentation with the goal to identify the crucial players in determining cell mechanics is challenging. Mutational or pharmacological modifications of the cell wall biochemistry often result in pleiotropic effects through feedback mechanisms that

---

ADVANCES

- Polar cellular morphogenesis of pollen tubes and trichome branches involves isotropic cell wall structure at the apex, whereas the shank is transversely reinforced ensuring a tubular geometry.
- Self-similar growth of pollen tubes entails a gradient of elastic modulus increasing from tip to shank. Growth/strain anisotropy in a trichome branch is correlated with an attenuating cell wall thickness or elastic modulus toward the tip.
- Finite element (FE) modeling has been used to predict the locations of elevated stress in pavement cells revealing spatial overlap with incidences of enhanced microtubule bundling. These FE models have also been employed to assess how tissue-level cues compete with subcellular stress.
- Formation of undulations in pavement cells is proposed to involve alternating material stiffness in the anticlinal walls.
- The opening mechanism of stomatal guard cells has been suggested to involve the geometry of the cell cross-section, radial cellulose reinforcement, local variations in pectin composition, and polar restriction of expansion.

---

alter other cellular processes. Therefore, mechanical modeling has proven useful to guide biological experimentation by focusing on mechanical aspects of the behavior. Most modeling approaches in plant cell mechanics are based on the premise that the cell wall is a deformable material and that the deforming force is the turgor pressure, uniformly applied within the compartment of a single cell. This concept applies both to irreversible shape changes (cell growth) and reversible shape changes (stress generation or turgor-regulated motion). Since turgor is a scalar, for nonspherical cell shapes to develop during differentiation, the cell wall mechanical behavior must differ between subcellular regions. This can be achieved through the variation of wall thickness or heterogenous distribution of the material properties (Green, 1962; Sanati Nezhad and Geitmann, 2015). The mechanical aspects of shaping or deformation processes can be explored using a variety of mathematical approaches (Dyson and Jensen, 2010). The finite element (FE) method is one of the available computational techniques particularly suitable for the analysis of problems in continuum mechanics with a high degree of geometrical details or material complexity (Box 1). This Update analyzes examples in which this numerical tool is applied to evaluate the growth and elastic deformations of individual plant cells.

The uses of FE modeling for cell or tissue studies can be categorized as forward or inverse approaches. The forward use of a model describes a deformation behavior, reversible or irreversible, inherent to the cell, such as a growth or shaping process. The purpose is to predict or explain the mechanical behavior arising from wall properties and turgor pressure (Fig. 1). Models used for an inverse approach are employed for the identification of material parameters from experiments such as indentation measurements (Bolduc et al., 2006; Bidhendi and Korhonen, 2012; Forouzesh et al., 2013; Sanati Nezhad et al., 2013). In this Update, we take a critical look at selected forward modeling studies of single plant cells (Fig. 1).

IRREVERSIBLE SHAPE FORMATION IN GROWING PLANT CELLS

Plant cell growth involves an irreversible stretching of the cell wall and an increase in cell volume and surface that can be substantial in certain cell types. Biologically, this is accompanied by the continuous insertion of new cell wall material to the existing wall. Simulating the resulting large deformations and the concomitant addition of material is a challenge for mechanical modeling that can be tackled in several ways. Typically, when using FE modeling, small, pressure-induced deformations are simulated repeatedly, and between the increments, a remeshing is performed. The geometrical structure resulting from the previous deformation step is meshed again to replace the often distorted mesh from the previous step.

BOX 1. Process Involved in Establishing a Finite Element Model

Constructing a finite element model entails four principal steps. First, the geometry of the problem is defined (Fig. 1A). The structure is then meshed by discretizing the geometry into a finite number of subdomains called elements (Fig. 1B). Each element is defined by nodes at vertices. Then, boundary conditions are imposed on the model to define and constrain the behavior of the structure properly. Boundary conditions are values, such as displacements, that are defined for certain nodes, such as those at external borders of the structure (Fig. 1C). Displacements, interactions between bodies, and external forces applied to the system are defined at this step. FE allows for the definition of complex interactions between bodies, such as friction or fluid flow at the boundaries. Different load types can be imposed on the model, such as pressure, concentrated or distributed forces, or gravity (Fig. 1C). The final step is to assign a material model to the elements of the structure that explains how the material behaves under loads (Box 3). Upon running the simulation, the FE algorithm constructs a stiffness matrix relating the forces and displacements for each element. The matrices of all elements are assembled into global matrices for the whole model. Applying the boundary conditions and inverting the global stiffness matrix yield the load-induced displacements for each node from which various outputs such as strains and stresses are computed (Fig. 1D).

Stretching of the cell wall due to loading results in a reduction of cell wall thickness. To account for the addition of new material, the thickness of the wall is readjusted (e.g. set to the initial value to maintain a constant wall thickness). This principle has been used, for example, to simulate tip growth in the pollen tube, the delivery organ for the sperm cells in plants (Fayant et al., 2010).

FE Modeling of Tip Growth

Tip-growing cells such as pollen tubes, root hairs, and fungal hyphae feature a spatially confined expansion zone allowing these cells to perform invasive behavior (Sanati Nezhad et al., 2013; Sanati Nezhad and Geitmann, 2015; Bascom et al., 2018). The profile of
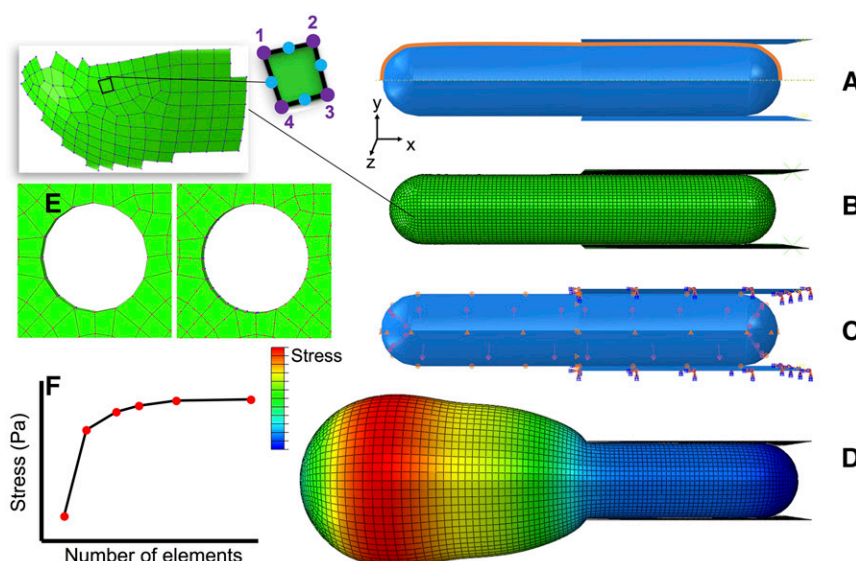
Figure 1. A, A closed cylindrical shell with hemispherical caps generated by the rotation of a line (orange) around a symmetry axis (yellow). The thin-shelled closed vessel is constrained on its right half by two nondeforming rigid, flat plates. B, The cylinder is meshed using three-dimensional quadrilateral shell elements (curved shell). The image on the left shows the first-order elements defined by four nodes (purple) used to discretize the geometry. Additional nodes (blue) would formulate the second-order elements. The elements can be regularly shaped or skewed. Excessively skewed element shapes are to be avoided. C, Boundary conditions are applied to the model. The rigid plates are fixed to prevent their rotation or displacement. Displacement boundary conditions are applied to prevent the cylinder moving freely in the space. The turgor pressure is applied uniformly to the internal surfaces. A sliding frictionless contact property is defined between the rigid plates and the deformable cylinder to prevent the penetration of one body into the other, while allowing their relative displacement. D, The isotropic closed cylinder deforms toward a spherical shape where it is not constricted by the plates. The heat map represents the von Mises stress distribution. E, First-order (left) and second-order (right) elements used around a discontinuity. F, Graph depicting the results obtained in a mesh convergence study. A value such as stress in a critical region is plotted against the total number of elements representing the structure to verify the independence of results from the mesh quality and the number of elements.

the growing tip is radially symmetrical and remains self-similar when moving forward. Mutations or pharmacological treatments interfering with cytoskeletal functioning or cell wall composition can affect the self-similarity, resulting in either a tapered or a swollen phenotype (Kost et al., 1999; Hwang et al., 2005; Klahre et al., 2006; Kost, 2008). Modeling of tip growth has been addressed using a variety of approaches (Goriely and Tabor, 2003; Dumais et al., 2006; Kroeger et al., 2008; Campàs and Mahadevan, 2009; Kroeger and Geitmann, 2011, 2012), one of which focused on the cell wall mechanical properties using the FE approach. FE modeling was used specifically to simulate how the generation of aberrant pollen tube phenotypes is mediated by changes in the cell wall mechanics (Fayant et al. (2010). The wall of the growing pollen tube was represented with a shell of uniform thickness (Box 2) but spatially varying material properties. The apical dome was divided into hoop-shaped subregions in which the elastic modulus (Box 3; Boudaoud, 2010; Dumais, 2013; Niklas, 1992; Huang et al., 2012; Julkunen et al., 2007; Kha et al., 2010; Sun, 2006; Zerzour et al., 2009) could be assigned independently (Fig. 2A). Load application was performed repeatedly, and after each step, the structure was remeshed, and the wall thickness was reset to the initial value to counter thinning and simulate the addition of cell wall material (Fig. 2B). The goal was to predict the spatial distribution of material properties in the cell wall that would generate perfectly cylindrical and self-similar growth patterns and to identify those that result in deviations such as swelling and tapering.

Two types of biological constraints were used to validate the biological relevance of the simulations. To represent a normally growing tube, the model had to produce a self-similar shape profile, and the strain pattern resulting from the deformation of the wall had to reproduce those observed experimentally (Rojas et al., 2011). Two key mechanical parameters were analyzed for their ability to shape the tube: (1) the profile of the elastic modulus gradient from tip to shank; and (2) the degree of material anisotropy expressing how different the material responds to loads applied in different directions. The validation suggested that isotropic behavior combined with a characteristic increase in elastic modulus, gradual from the tip to the flank and sudden from the flank to the shank, most accurately reproduce the pollen tube growth pattern. The mechanical gradients incorporated in this model were implemented as varying the elastic modulus between

BOX 2. Geometry, Elements, and Meshing

The geometry of a finite element structure can be produced either by parametric drawing using a computer-aided design (CAD) software or reconstructed from sample images, e.g. from a 3D confocal stack. Simplification is a crucial consideration. Any feature that is not a part of the simulation or is not likely to affect the outcome is removed to minimize model development and computation times. For instance, symmetry about an axis can be exploited to model the 3D problem as a 2D axisymmetric model or shape symmetry can be exploited to model only a portion of the geometry. However, discretion is required to avoid eliminating any relevant information in this process.

The plant cell wall is usually represented as either a "shell" or a "solid" model. In the "shell" approach, the thickness of the wall is an input value while in the "solid" approach, it is directly reflected by the 3D geometry. Shell idealization is appropriate when the thickness of the cell wall is negligible compared to other dimensions (e.g. local radius of curvature). This is the case for a typical primary cell wall of 100–500 nm thickness compared to a typical cell diameter of 10–50 μm. If detailed information on stresses or strains through the thickness of the wall is needed, however, a "solid" approach using volumetric elements is more appropriate.

Elements discretizing the body can be one-dimensional beams, two-dimensional triangles or quadrilaterals, or three-dimensional elements, depending on the dimensions and curvature of the structure. Elements can be of first, second, or higher orders. Second-order elements, for instance, have additional midside nodes (Fig. 1B). The choice of the element type,

is a critical step since it affects the computation time and the precision of the calculations. For instance, additional nodes in second-order elements, for the same number of elements, allow capturing the curvatures better (Fig. 1E). Therefore, there is often a compromise between using fewer second-order or more first-order elements. Similarly, shear-locking or overly stiff behavior in some of the first-order elements formulations is alleviated in quadratic elements, which enables them to calculate the deformations and stresses more accurately in bending-dominated applications (Sun, 2006). Nodes possess degrees of freedom that describe their properties. In the simplest form, this defines the displacement possibilities of the node in 2D or 3D space. In special applications, additional degrees of freedoms such as pore pressure or temperature are added. The size of the elements discretizing the geometry is adjusted based on the resolution of the solution needed. While the precision can be increased by refining the element size, in practice, due to limitations such as computation time, elements are refined only locally in critical regions. These include zones where a more precise solution is needed, around discontinuities or contacts with other bodies. A mesh convergence study must be carried out to ensure that the solution of a simulation is not dependent on the number and quality of elements used. For this purpose, the number of elements is increased iteratively, and the results (e.g. critical stress at a specified location) are compared until the variation in the solution is deemed negligible (Fig. 1F).

discrete regions rather than as a continuous and smooth function, and the values extracted were rather approximate. Despite these approximations, the model results matched well with mechanical and biochemical

observations, suggesting that the simplification was not detrimental to the purpose of the study. Crucially, the gradient in elastic modulus predicted by the FE model correlates well with the biochemical composition of the

Figure 2. A, A pollen tube modeled as a hollow shell with uniform thickness. The apical dome is divided into subregions, allowing for the elastic properties to be adjusted in each region independently. B, Several key points are followed on the FE model upon each loading cycle and remeshing to mimic growth. C, The stiffness gradient predicted by the FE model to produce a self-similar tube closely matches the deesterification pattern of pectin. Images were adopted from Fayant et al. (2010).
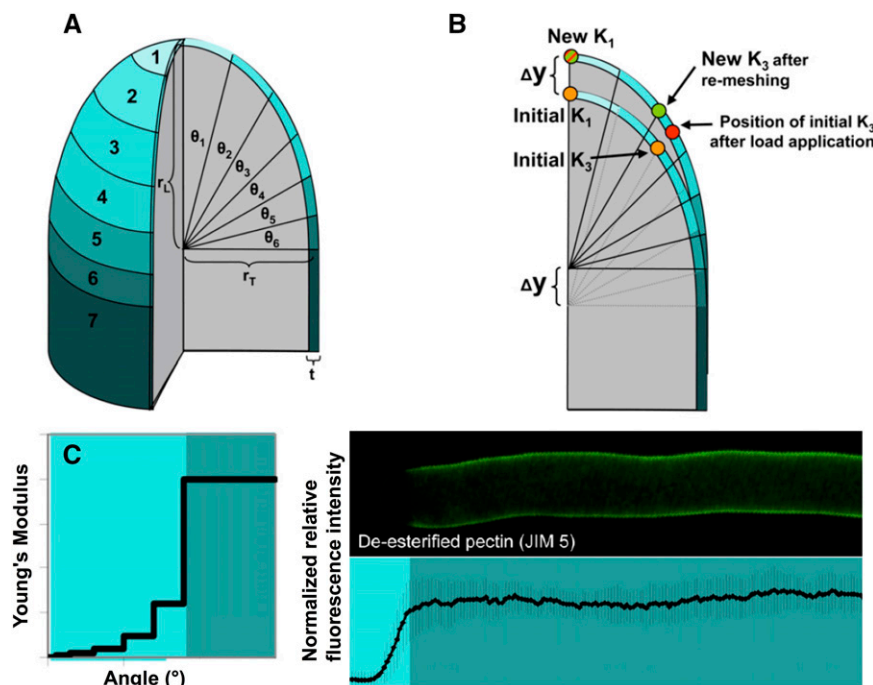
BOX 3. Material Models

Some of the basic concepts in mechanical behavior of materials such as deformation due to loading, stress and strain, creep or relaxation, elasticity or plasticity and parameters, such as Young's modulus and Poisson's ratio, are covered in helpful reviews (Niklas, 1992; Geitmann and Ortega, 2009; Boudaoud, 2010; Dumais, 2013). The material model to describe plant cell mechanics can be linear or nonlinear. This choice depends on the problem being solved. When large deformations occur in the model, as in the simulation of growth, a nonlinear elastic material model (e.g. a hyperelastic formulation) is preferable. Time-dependent properties, such as viscoelasticity, can be incorporated using information gained from mechanical tests, such as creep or relaxation. One of the simplest hyperelastic formulations is the Neo-Hookean model that requires defining only two material inputs. This is analogous to isotropic linear elasticity that requires two Lamé constants, such as Young's modulus and Poisson's ratio, to be defined. While using material models with a greater number of constants sometimes helps to achieve a better fit to an experimental observation, the lack of uniqueness of model parameters that can replicate an experimental observation can make the model unsuitable for producing meaningful predictions. If material models with several independent parameters are used to define the mechanical behavior of the cell wall, several types of experiments or simplifying assumption are needed to ensure their uniqueness. Mechanical anisotropy is an important property that can be incorporated to explain the behavior of the cell wall. This parameter characterizes how the material behaves in various directions. A fully anisotropic behavior (different properties in any given direction) is impractical to define due to the many parameters required. Therefore, if suitable, material symmetry (this differs from geometrical symmetry in Box 2) is often used to idealize the material behavior. Among the useful idealizations are transverse isotropy (isotropic properties in a plane perpendicular to the axis along the fiber direction) or orthotropic behavior (with three perpendicular planes or axes of material symmetry). Transverse isotropy, for instance, is very well-suited to represent the anisotropy of the cell wall due to preferential orientation of cellulose microfibrils. Such anisotropic cases are defined by assigning different material constants along independent coordinate directions. A promising approach adopted for plant cell wall material was the use of hyperelastic models, such as the Holzapfel-Gasser-Ogden model (e.g., Gasser et al., 2006) that allow for separate definition of fiber (e.g., cellulose) and matrix (e.g., pectin) phases. This model, in particular, has been used to formulate the transverse isotropy of plant cell wall material (Huang et al., 2012; Yanagisawa et al., 2015). User-defined materials can be developed and incorporated into the FE model definition to account for any further detail in behavior or interactions between cell wall constituents (e.g. refer to Julkunen et al., 2007; Kha et al., 2010; Yi and Puri, 2012).

pollen tube wall, notably the distribution of esterified and acidic pectin (Fig. 2C). This result is consistent with the effect of the pectinase-mediated digestion of pectin, which results in a dramatic apical swelling of the pollen tube (Parre and Geitmann, 2005), presumably through the loss of the modulus gradient. It also accords well with mechanical measurements revealing that the cell wall at the tip of the growing pollen tube is softer and modulates its properties to generate an oscillatory growth pattern (Zerzour et al., 2009). The reciprocation between predictions made by the in silico FE model, experimental validation, refinement of the model, and guidance toward further biological experimentation illustrates the value of FE in the predictive modeling of cell development.

FE Modeling of Diffuse Growth during Trichome Branch Morphogenesis

A similar yet distinct modeling approach was carried out to investigate the growth mechanics in trichomes. These epidermal cells (Fig. 3A) come in many shapes, sizes, and metabolic functions. They can be branched or unbranched, glandular or nonglandular (Tissier, 2012), and can be single-cell entities or comprise multiple cells. Trichome shape is intimately linked to their respective function, such as defense, pollination, or moisture retention (Oelschlägel et al., 2009; Amada et al., 2017). The unicellular trichome in Arabidopsis (*Arabidopsis thaliana*) forms a stellate body with three or four branches and is an excellent cell type in which to investigate the mechanics underlying complex cell morphogenesis. Actin is involved in the diffuse growth of plant cells (see Szymanski and Staiger, 2018). Disruption of cytoskeletal components is associated with the loss of branching, a needle-like phenotype, or swelling (Mathur et al., 1999; Szymanski et al., 1999; Mathur, 2004), phenotypes that can be studied using FE modeling. Branch morphogenesis in Arabidopsis trichomes was investigated using FE modeling in conjunction with live-cell imaging to understand the mechanics of branch growth (Yanagisawa et al., 2015). Similar to modeling of the pollen tube, the two constraints on the model to match were the shape of the branch and the growth (strain) pattern of the wall. Time-lapse imaging demonstrated that, unlike the self-similar pollen tube, the trichome tip radius tapers off while the radius of the base of the branch remains relatively constant (Fig. 3B). Fiducial markers were used to track the local growth pattern. To justify a choice of material model, the authors visualized the alignment of cellulose synthase (CESA) complexes and microtubules (see Elliott and Shaw, 2018), which were oriented transversely to the branch axis. Motivated by this preferential orientation inferred for cellulose that is commonly regarded as the major load-bearing polymer of the cell wall, transverse isotropy (Box 3) was incorporated in the elastic model using the Holzapfel-Gasser-Ogden
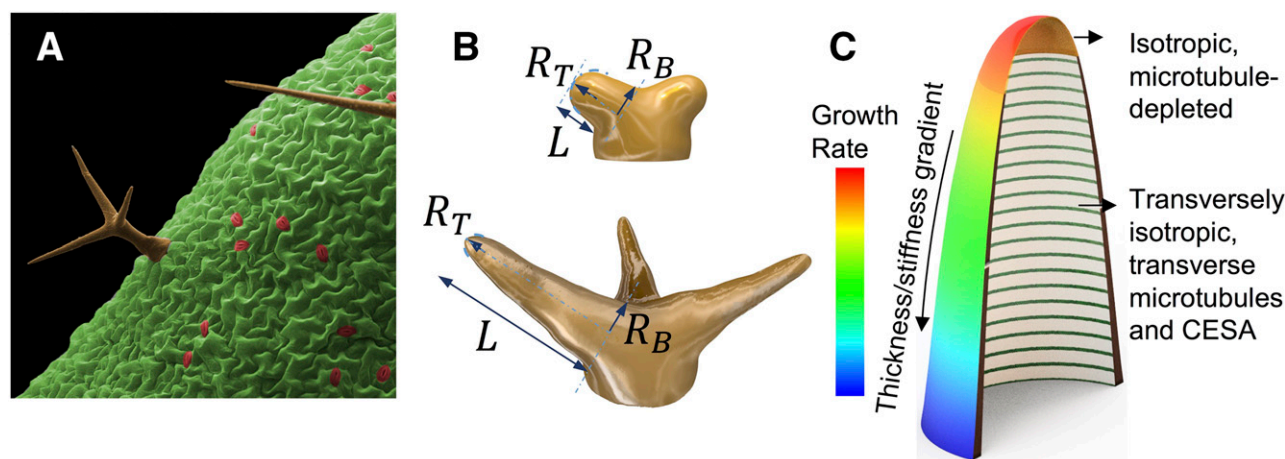
Figure 3. A, Epidermal cells on the adaxial surface of an Arabidopsis leaf feature three cell types: trichomes (brown), stomatal guard cells (red), and pavement cells (green). B, Development of the trichome branch embodies reduction of the tip radius of curvature, while the radius at the base of the branch remains constant. L, branch length; RT, branch radius at the tip; RB, branch radius at the base. C, The growth and thickness of the cell wall in a trichome branch are correlated and exhibit a gradient toward the tip of the branch. Microtubules and CESA trajectories are oriented transversely to the long axis of the branch, while the tip exhibits a microtubule-depleted zone. Image redrawn after Yanagisawa et al. (2015).

hyperelastic material behavior (Gasser et al., 2006). The critical parameters in this material model are the dispersion, fiber angle, and fiber-to-matrix stiffness ratio, which needs to be sufficiently large for anisotropy to emerge (Huang et al., 2012). The FE simulations indicated that strong transverse alignment of fibers results in the anisotropic, axial growth of the shell. The random orientation of the fibers implemented in this model produced a spherical bulge instead.

As the tip apex of the trichomes was observed to be depleted of microtubules, it was concluded that the cell wall at the tip should be isotropic. Varying the size of the isotropic zone and comparing the evolution of the tip radius of curvature against the branch length, the FE results indicated that the size of the isotropic apical zone should vary over time to reproduce the experimentally observed tapering. This conclusion was drawn because no single value of the tip isotropic zone could produce results that fit the experimental curve. It is not clear to what extent such detailed results depend on the choice of material model, and whether a different hyperelastic model would bear a different conclusion remains to be investigated. However, the transverse isotropy per se could not reproduce the growth gradient toward the tip observed experimentally (Fig. 3C). Therefore, it was suggested that a thickness or elastic modulus gradient should exist along the trichome branch. Transmission electron microscopy and light microscopy confirmed this predicted attenuation of cell wall thickness toward the tip, with a value close to but less dramatic than that predicted by the FE model. Therefore, a combination of both thickness and elastic modulus gradient parameters might be employed by the cell, although the FE model used here produced unrealistic results when combining the two. As

remarked earlier, it would be interesting to investigate the dependency of simulation results on the material model employed.

In the Arabidopsis mutant *arpc2/distorted2*, trichome branch growth is hampered, the tip radius of curvature remains high compared with the wild type, and the stalk swells (Kotchoni et al., 2009). Intriguingly, wall thickness and growth gradients were both absent in these aberrant trichome branches, further corroborating a correlation between wall thickness and growth rate variations. However, whether the relationship is causal, and if it is, which is the cause or effect, remain unclear. While a thinner wall in the model can translate into a lower rigidity to reproduce a higher strain, a higher strain in the absence of reinforcing new wall material results in wall thinning. Likewise, the absence of a thickness gradient in *arpc2* may result from a failure to grow and a consequent lack of wall thinning. This study suggests that, while similarities exist, the growth behavior particular to trichome branches is distinct from tip growth, as the tip radius attenuates, wall thickness is not preserved, and growth occurs in the whole branch rather than a confined apical zone. Yanagisawa et al. (2015) report that the cell wall of *arpc2* is enriched in well-aligned cellulose, and microtubules are transversely oriented. Cellulose orientation was used as a proxy for transverse isotropy bringing about anisotropic (axial) growth in mutant branches. Although trichome branches in *arpc2* do not grow considerably, comparing the time data provided for the branch length and tip radius for the wild type and mutant shows that, for an equal length (e.g. at 40-μm branch length), the mutant branch has a larger tip radius of curvature, indicating that at least some degree of swelling occurs in the branch too, besides the general swelling in the stalk

(see Figs. 1B and 3C in Yanagisawa et al., 2015). Whether this apparent swelling is a result of changes in the tip isotropic zone or changes in other wall polymers is not clear. While the fibrillar texture of the cell walls between the wild type and the mutant seems unaltered, the quality of the fibers and their linkages might have undergone changes. Furthermore, other wall polymers may have been affected as a result of mutation. This emphasizes the need for experimental studies to characterize and compare the changes in mechanical properties in a wide array of Arabidopsis mutants; the mechanical changes due to mutations can be manifested in ways that go beyond what can be assessed readily by visually tracing cellulose orientation.

In the studies that have modeled the shaping process of plant cells using the FE method, the geometry is loaded incrementally while cell wall thickness is adjusted to account for the addition of material. The drawback of this strategy is that this process results in the elimination of stresses that develop in each increment. While it is possible to retain the stress information and transfer it to the next increment, it might differ from the quality of wall stresses during the insertion of wall-building materials. Attempts to describe cell growth were also been done by using viscoelastic behavior (Huang et al., 2015). However, loading to deform an elastic or viscoelastic structure develops stresses that cleavage of chemical bonds and insertion of new materials might not. In fact, currently, we have little information on changes occurring in cell wall stress during growth or cell deformation. Additionally, in most of the available modeling studies, stress information is presented only in relative form. Absolute stress values could serve as a useful parameter to further validate the quality and relevance of a model's predictions. However, reporting absolute values based on models that are inevitably greatly simplified requires considerable experimental support, as explained below.

Stress Development in Plant Cells Correlates with Morphogenetic Phenomena

A subset of forward FE simulations of plant cells are the stress analysis models. The main parameter investigated in these models is generally the stress developed in a single step of turgor application. The stress analysis models of plant cells or tissues published so far do not fall under irreversible FE models and are static, since they do not involve remeshing, wall modification, stress update, or otherwise introduction of a form of permanent deformation. While these models do not explicitly simulate irreversible material deformation, since they are sometimes employed to investigate the link between the mechanics and a physiological or morphogenetic response, such as cytoskeletal patterning, that can be linked to an irreversible biological response, we categorize them under the irreversible use of FE models. Several studies use static stress analysis to correlate the mechanical aspects with a morphogenetic problem such as gene expression, hormonal activity, and ontogeny at tissue scale (Bassel et al., 2014; Bozorg et al., 2014; Boudon et al., 2015). To illustrate the concept, however, here we will discuss those that focus primarily on cell shape, namely the shape of epidermal pavement cells in relation to microtubule organization and wall biochemistry. Pavement cells in the leaf epidermis of eudicotyledons form interlocking patterns similar to pieces of a jigsaw puzzle (Fig. 3A). There have been numerous hypotheses, such as cuticle stiffening or cells being squeezed physically during growth, to explain the peculiar shaping phenomenon in these cells (Korn, 1976; Armour et al., 2015). The potential role of mechanics underlying the shaping process and the potential advantages of such cell shape for the epidermis or leaf have remained elusive (Jacques et al., 2014). Since pavement cells, as opposed to trichome branches, are tightly connected to neighboring cells, they allow studying the mechanics of cell-tissue interaction. Studies have suggested the involvement of the cytoskeleton in the shaping process downstream of an auxin-dependent pathway (Fu et al., 2005; Xu et al., 2010; Zhang et al., 2011; Lin et al., 2013). Microtubules are suggested to be associated with regions of indentation (often termed the neck), putatively resulting in anisotropic reinforcement of these regions by guiding CESA complexes and preferential deposition of cellulose microfibrils (Panteris and Galatis, 2005; Belteton et al., 2018). For simpler cell shapes, it is known that microtubules reorient in the direction of maximal mechanical stress (Williamson, 1990; Hamant et al., 2008). Whether the microtubule arrays experimentally observed in pavement cells equally correlate with stress patterns, however, was unknown for lack of information on stress distribution.

### FE Modeling of Turgor-Induced Stresses in the Periclinal Pavement Cell Walls

The correlation between cell shape, mechanical stress, and microtubule alignment can be easily verified for simpler cell geometries, such as the tubular shapes of trichome branches or root and shoot epidermal cells. In a pressurized thin-walled cylindrical vessel with hemispherical caps, the pressure-induced transverse stress that arises due to cell shape is twice the longitudinal component. However, in the case of pavement cells, predicting the local distribution of stress is not as straightforward. Sampathkumar et al. (2014) used FE modeling to study the effect of cell shape and tissue-level stresses on microtubule arrangement in pavement cells. The static model developed in this study focuses on cell-level stress development and how it correlates with tissue-level mechanical and physiological responses. The FE model consists of the outer periclinal walls (the horizontal walls parallel to the plane of leaf) of pavement cells, extracted from confocal microscopy stacks, modeled as thin shells. At the borders of

periclinal walls, the anticlinal walls (the vertical side walls) were modeled as 1D beam elements adding stiffness to borders. Tensile stress was generated in the cell walls upon the application of pressure to the inner face of the walls. Whether an isotropic or transversely isotropic hyperelastic material was used, the result indicated a higher stress at the indentation side of the wavy borders. The location and pattern of stress from the shell FE model matched well with the anisotropic alignment of microtubules, with a preference for bundling at sites of indentation (Fu et al., 2005; Zhang et al., 2011; Armour et al., 2015). These data suggest that stress resulting from cell shape at the subcellular scale might act as a mechanical cue for the cytoskeletal arrangement, even in cells with complex shapes.

Sampathkumar et al. (2014) used the FE model of the pavement cells further, to predict the microtubule organization based on tissue-level stress patterns and their alterations upon the application of external forces or cell ablation. The FE model suggested that, upon laceration, or more subtly, cell ablation, the stress pattern becomes circumferential around the vacant region (Fig. 4, A and C). Cell removal was reproduced in the model by gradual reduction in turgor pressure and cell wall stiffness in compromised cells. Time-lapse imaging reported an increase in microtubule bundling and a change in organization hours after laceration. Previous observations also had reported a reorientation of microtubules due to externally applied mechanical stress in Arabidopsis leaves (Jacques et al., 2013). The authors propose that this indicates that changes in tissue-wide mechanical stresses can affect microtubule organization despite the initial cell-level order imposed on microtubular arrangement. However, to what degree the perturbation of mechanical stresses at tissue scale can override the cell-level control of microtubule arrangement is disputable. First, the FE model developed by Sampathkumar et al. (2014) predicts that, upon laceration or cell removal, circumferential stress patterns would be produced in pavement cells in a region of tissue spanning over multiple cells (Fig. 4A). Conversely, observation of a fluorescently tagged microtubule line seems to suggest that microtubule arrangement is affected more strongly only in cells near the afflicted region (Fig. 4B). Second, the study reports that the response of microtubules to changes in mechanical stress depends upon the magnitude of stress. To demonstrate this, the FE model was used to reproduce the ablation of only a few pavement cells. Similar to the case of laceration but with a lower magnitude, the FE model predicts a circumferential rearrangement of microtubules adjacent to the location of the perished cells (Fig. 4C). However, the experimental observation does not seem to closely match the FE prediction (Fig. 4, C and D). The authors argue that this observation demonstrates a stress-magnitude dependency of the microtubule

Figure 4. A, FE model suggesting a stress pattern in pavement cells circumferential to the site of laceration. B, Fluorescence-tagged microtubules demonstrate hyperbundling and a seemingly circumferential pattern around the wound site. White arrowheads show examples of noncircumferential microtubules in cells away from the site of laceration. The white arrow shows that, even in cells adjacent to laceration, there seems to be a local competition between the cell shape-dictated microtubule organization and the putative circumferential reorientation of microtubules due to tissue-level stress. C, FE model suggesting a stress pattern in pavement cells circumferential to removed cells. D, Microtubules demonstrate a change in bundling and orientation upon the small-scale wound. However, their orientations seem longitudinal to cell axes rather than being circumferential to the site of the wound. White arrows indicate examples of cells with microtubules oriented parallel to the long cell axis, inconsistent with the hypothesized circumferential orientation. The star indicates ablated cells. Numbers indicated individual cells. All these images are reprinted from Sampathkumar et al. (2014) with permission from the authors. Bars = 25 μm (B) and 50 μm (D).
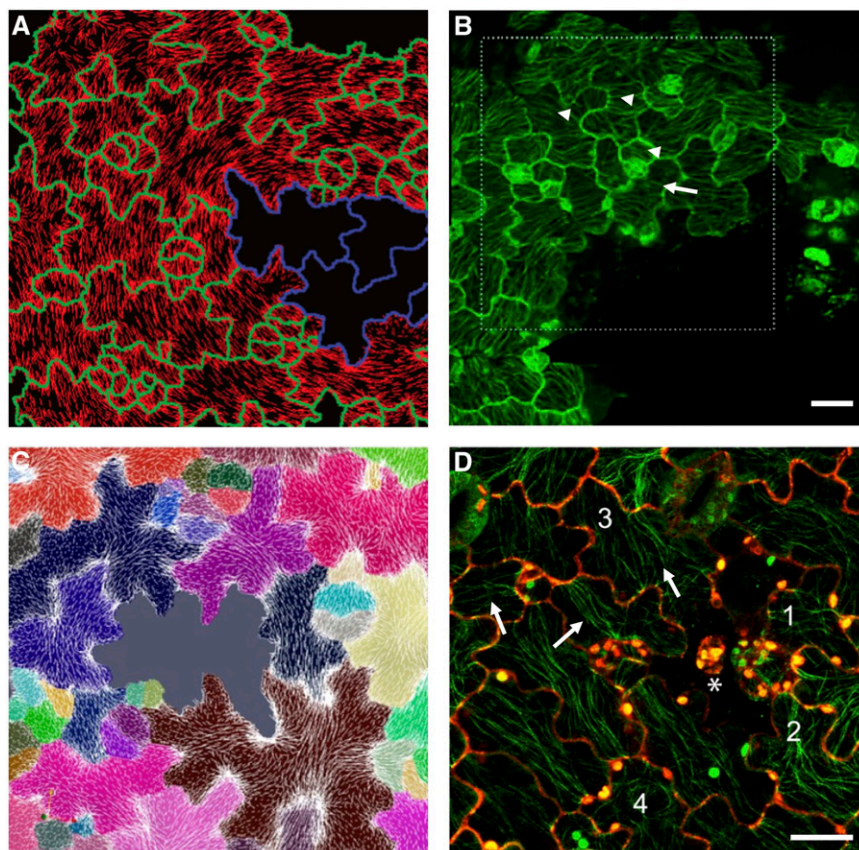
rearrangement and that ablation of only a few cells does not seem to be able to strongly rearrange the microtubules circumferentially in neighboring cells. However, a closer look reveals microtubules in neighboring cells to be oriented predominantly parallel to the long axes of the cells, rather than featuring a circumferential orientation around the site of ablation (Fig. 4D). This might indicate that the rearrangement of microtubules due to cell ablation might at least partially occur due to other cues, such as a wound response, a mechanism shown previously (Geitmann et al., 1997). Furthermore, the microtubule response might depend upon a competition between the subcellular and supercellular cues, with a weight factor for each that depends on the homeostasis within the cell and tissue, rather than being dominated consistently by one.

FE Modeling of Wave Formation in Anticlinal Walls of Pavement Cells

While the model by Sampathkumar et al. (2014) was useful to predict how stresses in fully differentiated pavement cells are distributed, it does not address the generation of the cell undulations. Majda et al. (2017) proposed an FE model to explain the underlying mechanics of wave formation in pavement cells. Motivated by their undulating shapes, the model focuses exclusively on the anticlinal cell walls. The authors propose that wave formation results from bending of the anticlinal walls due to their stretching combined with a particular spatial distribution of mechanical properties. The FE model developed in this study purportedly demonstrates that, if segments with high and low elastic moduli are laid alternatingly along and across the anticlinal walls, stretching this structure forms bends resembling the protrusions and indentations of the pavement cell wall. A main result of the model is that the indentation side of the bend of the anticlinal wall is associated with the softer material. While this result seems corroborated by the atomic force microscopy (AFM) stiffness measurements reported in this study, it is challenged by available data on the mechanics of the pavement cell wall. First, as mentioned before, well-aligned microtubules are associated with indentation sides in anticlinal and periclinal walls (Fu et al., 2005; Zhang et al., 2011; Armour et al., 2015), although whether these antecede the initiation of undulations warrants further investigation (Belteton et al., 2018). It was hypothesized that this microtubular array leads to the deposition of well-aligned cellulose enrichment, thus preventing further expansion in these areas of the periclinal walls (Panteris and Galatis, 2005). This local stiffening in the periclinal wall of differentiated cells is corroborated by AFM stiffness mapping (Sampathkumar et al., 2014). Moreover, using fiducial markers on the surface of growing pavement cells, Armour et al. (2015) demonstrated that cell wall expansion is more pronounced on the protrusion side of undulations while the opposing indentation sides

seemed restricted in their growth. This further corroborates an added stiffness at the indentation side, all of which seems to be difficult to reconcile with the results of the anticlinal wall FE model developed by Majda et al. (2017).

While the two scenarios are not mutually exclusive, reconciling them would necessitate allowing for a drastic and sudden change in the biochemical and biomechanical makeup at the border between adjacent cell wall regions. An indentation would have to feature a stiff periclinal wall (Panteris and Galatis, 2005; Sampathkumar et al., 2014; Armour et al., 2015) directly neighboring a soft anticlinal wall (Majda et al., 2017). Only detailed analysis of the local wall biochemistry and mechanical behavior will provide conclusive answers. An additional consideration is the geometry. Given that the very narrow band of the anticlinal wall is bordered by two large sheets of periclinal wall, potentially representing significant boundary conditions limiting the freedom of displacement, one wonders whether the former can dominate the latter and whether modeling the anticlinal wall while entirely neglecting the periclinal walls can be a justifiable simplification. We posit that an FE model that represents the entire 3D geometry of the cell, including all its load-bearing walls, is warranted to address the challenge of wavy pavement cell morphogenesis.

REVERSIBLE SHAPE CHANGES IN PLANT CELLS

Reversible shape changes in plant organs and cells can be generated by modulation of the turgor pressure. As opposed to growth-related deformations, these remain mostly in the elastic range and do not involve dynamic modification of the cell wall material and biochemistry. However, these reversible movements are still governed by the mechanical properties of the cell wall material and the geometry of the cell or tissue. At the tissue level, the opening of the Venus flytrap (*Dionaea muscipula*) and processes enabling seed dispersal are examples of the exploitation of turgor modulation, cell shape, and wall mechanics to accomplish actuation (Forterre et al., 2005; Geitmann, 2016; Hofhuis et al., 2016). Similarly, motion at the single cell level, such as stomatal opening and closing, is powered hydraulically.

To illustrate the application of FE modeling to reversible shape changes, the example of stomatal guard cells is examined here. Guard cells form pores in the leaf epidermis that are specialized to optimize gas exchange between the plant and the environment. The ability of these epidermal valves to respond efficiently to various stimuli, such as light and aridity, is crucial for photosynthesis, water retention, and, thus, survival. Stomatal opening is driven by an increase in turgor pressure in the guard cells. The pressure in subsidiary cells, the specialized epidermal cells immediately surrounding the guard cells, antagonizes this process, together regulating the stomatal dynamics (Von Mohl, 1856;

Edwards et al., 1976; Franks and Farquhar, 1998). The shape and structure of guard cells vary among species. Stomata in graminaceous monocots have guard cells that are typically narrow and dumbbell shaped, whereas those of dicots are kidney shaped. Here, we focus on the latter. The increase in the width of the stomatal aperture by inflation of the guard cells is suggested to occur in two stages. The guard cells in the closed state of the pore display a nearly elliptical cross-section that becomes circular when pressurized (Fig. 5A). The first stage of the pore opening or increase in volume of guard cells is suggested to be governed mainly by an inflation-driven change in the cross-sectional shape of guard cells with little stretch in the wall. The further increase in cell volume is attributed to stretching of the cell wall accompanied by its thinning and expansion at the poles (Sharpe and Wu, 1978). How the swelling of the two guard cells, their specific design, and their wall mechanics enable pore opening has been the subject of multiple studies with somewhat antithetical outcomes (DeMichele and Sharpe, 1973; Raschke, 1975; Cooke et al., 1976, 2008; Sharpe and Wu, 1978; Amsbury et al., 2016; Carter et al., 2017; Woolfenden et al., 2017). Several cell features have been hypothesized to be critical for pore opening when guard cell pressure rises: (1) the increased thickness of the ventral walls of guard cells (Fig. 5A); (2) the radial reinforcement by cellulose microfibrils, resulting in anisotropy of the cell wall (Fig. 5B); (3) the elliptical cross-section of guard cells under low turgor pressure; and (4) the constraint on polar expansion of guard cells due to pectin deesterification.

Reversible Changes in Guard Cell Cross-Sectional Shape May Underlie Stomatal Pore Opening

FE studies by Cook and colleagues were among the first to consider a realistic closed-cell geometry for guard cells. The comprehensive analyses carried out in these studies produced results that remain cogent to date (Cooke et al., 1976, 2008; Lee, 1986; more information is available under Stomatal Control System [hdl.handle.net/1813/45423]). Cooke et al. (1976) modeled a generic stomate with a doubly elliptical toroidal shell by rotating an ellipse forming the transverse cross-section about another ellipse that lies in the horizontal plane (Fig. 5A; videos demonstrating the data for the guard cell model and results, for shell and solid, can be accessed at the following links: hdl.handle.net/1813/43793 and hdl.handle.net/1813/43794). The parameters investigated were the effects of guard cell geometry, wall thickness, radial cellulose reinforcement, and the turgor pressure in both guard and subsidiary cells. Thickening of the ventral wall has long been proposed to underlie pore opening (Meidner and Mansfield, 1968). Considering a nonuniform wall thickness, Cooke et al. (1976) found that opening of aperture width is virtually the same as in a model with uniform wall thickness, suggesting the wall thickness gradient to be insubstantial for stomatal opening. These
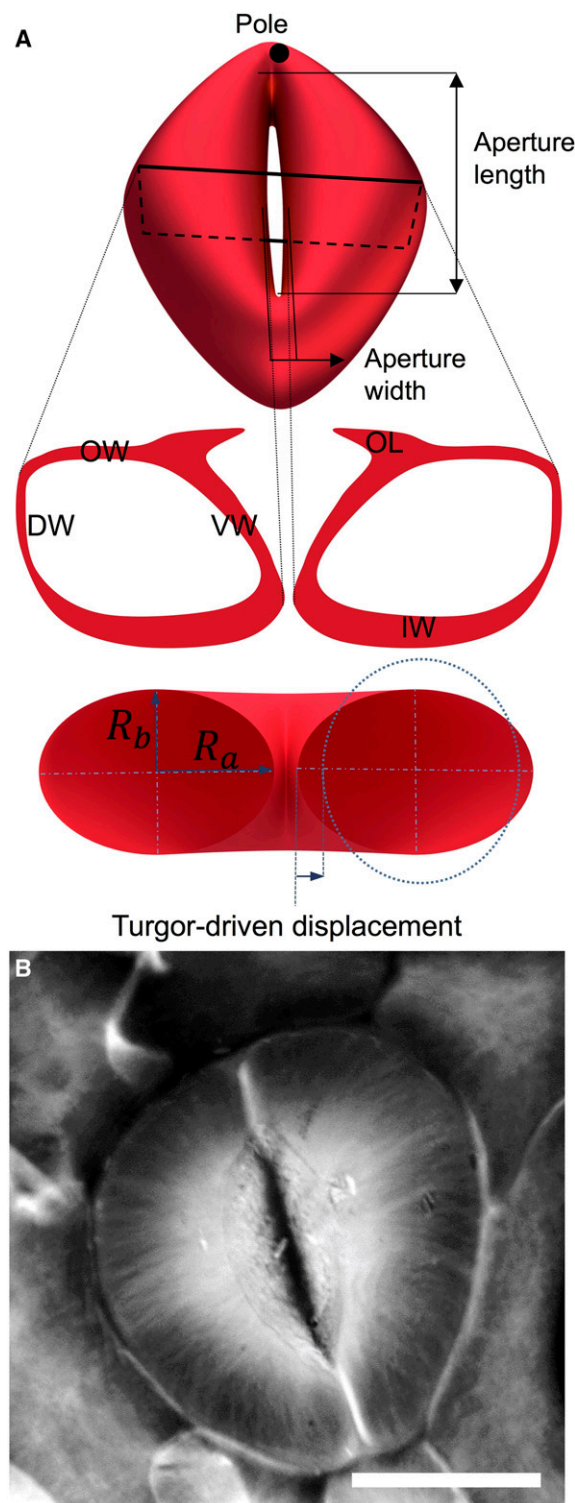

Figure 5. A, Cross-sectional view of guard cells composed of ventral wall (VW), dorsal wall (DW), inner wall (IW), and outer wall (OW). Ra and Rb refer to the horizontal and vertical radii of the elliptical cross-section, respectively. Only the outer ledge (OL) is shown. Inflation of the guard cells causes a change of the elliptical cross-section to circular and then to an ellipse with the major axis perpendicular to the plane of the leaf. B, Confocal micrograph of guard cells in an Arabidopsis cotyledon, stained with Calcofluor White to reveal cellulose. Bar = 15 μm.

results indicated, however, that the geometry of guard cells is paramount in their function. If the torus was set to be doubly circular in this model or if the cross-section was defined to be elliptical with the major axis perpendicular to the leaf (dotted ellipse in Fig. 5A), the pore was shown to close upon pressure application unless some physiologically implausible criteria were enforced. In these cases, the guard cell deformation majorly consisted of cell wall stretching rather than change in cell cross-sectional shape. In contrast to other geometries, the authors determined that a doubly elliptical geometry opens upon the application of turgor pressure and disturbs the neighboring cells minimally when inflated. The simulations indicated that, during deformation and pore opening, the cells bulge out of the leaf plane. While the width of the pair increases as a result of pore opening, the width of a guard cell can decrease slightly because of the out-of-plane bulge of the inner and outer walls. Interestingly, the aperture length was observed to remain virtually constant during pore opening, without necessitating a displacement restraint to be imposed a priori on guard cell poles.

Parametric studies carried out by Cooke et al. (1976) revealed that the aperture width is a multilinear function of the pressures in guard cells and subsidiary cells. An antagonism ratio was defined to express the contribution of each cell type in aperture opening. The radial orientation of cellulose microfibrils in mature guard cells (Fig. 4B) has long been known (Ziegenspeck, 1955), and the resulting transverse isotropy has been considered a crucial feature promoting stomatal opening. An early study even made a physical model of stomatal opening by radially reinforcing a pair of elongated balloons using adhesive tape (Aylor et al., 1973). In contrast, simulations by Cooke et al. (1976) suggest that circumferential cellulose reinforcement acts as a hindrance to aperture opening driven by guard cell inflation. *Ceteris paribus*, their model, predicted that increasing the elastic modulus of the wall in the radial direction, representing a higher anisotropy ratio by radial cellulose bundles, diminishes the effect of a unit increase in guard cell pressure on pore opening while it increases the contribution of a unit increase in the pressure of subsidiary cells in closing it. From this, the authors concluded that radial cellulose anisotropy is not a mechanism to open but, conversely, a leverage to close the pore. Interestingly, a recent study by Rui and Anderson (2016) has demonstrated that guard cells in a mutant with reduced cellulose content and anisotropy exhibit a wider aperture, which seems to, at least partly, support the findings of the model by Cooke et al. (1976), although assessing the dynamics of the pore opening and the effect of subsidiary cells will require further investigation. The emergence of such complex and nonlinear control on the Watergate by relying only on geometry and mechanics is a spectacularly simple strategy and may be, in part, how plants can respond rapidly and reliably to environmental cues (Roelfsema and Hedrich, 2005; Franks and Farquhar, 2007; Raven, 2014). Together, Cooke et al. (1976, 2008) and Lee (1986)

conclude that opening of the stomatal pore is influenced saliently by the elliptical geometry of the guard cell cross-section. They suggest that nonuniform wall thickening or anisotropic material properties are not required per se, although they might regulate the dynamic response of guard cells.

Reassessing the Contribution of Cellulose-Induced Radial Anisotropy to Stomatal Opening

The role of cellulose orientation and cell wall anisotropy was reassessed in a recent study by Woolfenden et al. (2017), who used nonlinear elasticity with a transversely isotropic material behavior to represent the guard cell wall, similar to studies by Cooke et al. (1976). The authors observed that, using isotropic material properties, increasing the turgor pressure causes the stomatal pore to close rather than open. A radially reinforced version of their model engendered pore opening. They concluded that circumferentially oriented cellulose microfibrils are crucial for stomatal opening. However, these results were based on a structure with an idealized circular cross-section for the guard cells, whereas the base model in the study by Cooke et al. (1976) was elliptical in cross-section (Fig. 5A). While Woolfenden et al. (2017) did simulate this situation as well, they stated that, at higher 'correct' pressures, the pore closes in the absence of anisotropic properties. The study does not explicitly state a caveat that cannot be neglected, however. Many of the model inputs, including the cell wall thickness, cross-sectional shape, and material model parameters including the elastic moduli, are significantly simplified, and idealized or arbitrary values are used, as is inevitable in the absence of biomechanical data. Therefore, it is hardly possible to expect the model to reliably predict anything more than general tendencies, even if biologically relevant absolute pressure values are used. A small change in, say, the assumed Young's modulus of the cell wall or the use of a different nonlinear elastic model has the potential to significantly alter the observed threshold values or even the trends at which the model switches from open to closed. Arguing that one model more accurately reflects the reality over another, if neither uses better quality input parameters, warrants substantiation. Similar caveats apply to attempts aimed at quantitatively identifying material constants from such models; many approaches are best suited to remain qualitative. This points to a limitation of modeling in plant cell mechanics in general. In the absence of detailed quantitative information, many parameters required to define the model must be input based on educated guesses, and whether the predictions made by the model hold in experimental conditions remains to be shown. That a given combination of material and geometrical parameters produces results resembling the biological situation is seducing but does not prove this combination to be the one reflecting the reality. Other solutions often are possible.

This caveat should at least be acknowledged but is not always done.

Another example is the observation that the aperture is least sensitive to turgor pressure at higher width (the curve moves toward a plateau; Franks and Farquhar, 1998). This led Woolfenden et al. (2017) to conclude that a strain stiffening must occur in the cell wall matrix. While this explanation is reasonable, it may not be the only one. Annexing increasing numbers of parameters to the model to match an observed behavior, without proper substantiation, risks appearing opportunistic if not arbitrary. The nonlinear behavior observed in experiments (Franks and Farquhar, 1998) also could be caused by a two-step opening mechanism, similar to the one described before and demonstrated in the FE model by Cooke et al. (1976, 2008). This would entail an initial turgor-induced change in geometry from elliptical to circular (inflation), followed by an accommodation of any further increase in pressure by cell wall stretching, a process that requires higher turgor differentials to produce visible results. Therefore, the matrix strain-stiffening conjecture proffered by Woolfenden et al. (2017), while consistent with polymer chemistry (Bidhendi and Geitmann, 2016), could be a secondary mechanism responsible for the apparent low sensitivity of aperture opening at high pressures. These concepts certainly merit further validation. Woolfenden et al. (2017), furthermore, did not extensively explore the effect of subsidiary cells in their model. They suggested that, in the presence of cellulose-mediated anisotropy in the guard cell walls, the effect of pressure in the subsidiary cells becomes negligible. This result is in clear contrast to that of Cooke et al. (1976), who reported the guard cell anisotropy to augment the effect of subsidiary cells in closing the stomata. Further investigations must address this discrepancy.

Correlating the Mechanics and Phenotype of Genotypes: The Devil May Lie in the Ultrastructural Details

While cell wall mechanical studies often focus on cellulose orientation, parameters such as cell wall thickness, cross-section shape, and other cell wall polymers seem to have the potential to influence the mechanics and function of guard cells. However, since a multitude of parameters may interplay, isolating the role of each may not always be straightforward. It has been reported that pectin chemistry is correlated with the ability of guard cells to function correctly (Merced and Renzaglia, 2014; Amsbury et al., 2016). *pme6-1* was shown to have a decreased dynamic range and a defect in stomatal opening. Interestingly, the results of immunolabeling suggest that, in wild-type Arabidopsis, unesterified pectin (antibody, LM19) is present in all cell wall regions of guard cells. Highly methylated pectin (antibody, LM20), on the other hand, is absent from guard cell walls, as also reported previously by Merced and Renzaglia (2014), and is limited to cell junctions, as is calcium-bridged pectin (antibody, 2F4). This means that

unesterified pectin in the guard cell walls, although negatively charged, does not seem to be gelated by calcium ions. In *pme6-1*, the pectin distribution was reversed: highly esterified pectin was reported in the entire guard cell wall. The authors concluded that pectin determines the mechanics of the cell wall and that lack of a functioning pectin methylesterase causes the wall to become too rigid and lose the deformability required to open the pore (Amsbury et al., 2016).

While this is a reasonable hypothesis (Bidhendi and Geitmann, 2016), the study provides no evidence for the fact that the weakly esterified pectin was gelated by calcium or whether the mechanical properties of the cell wall materials were altered in any way. The antibody 2F4 was not used on the mutant, let alone micromechanical testing of cell wall properties. More importantly, the study fails to ascertain that no other parameters are changed in the mutant. While the authors claim a lack of any noticeable difference in ultrastructure between the wild type and the mutant, transmission electron microscopy cross-section micrographs of the guard cells of *pme6-1* and the wild type provided in their study seem to reveal an interesting, yet conflicting, phenomenon (see Supplemental Fig. S2, G and H, of Amsbury et al., 2016). In cross-sections, the guard cell walls of the mutant appear considerably thicker than those of the wild type, relative to the area of the lumen. This seems especially the case for the inner walls. Whether the images in this paper are representative remains open. However, compensation mechanisms are common when a normal process of the cell is disturbed and can cause a chain of events. Here, in response to a disturbed function of pectin methylesterase, an increase in cell rigidity may have occurred through abnormal wall thickening. If this were confirmed, the change in cell wall dimensions or cross-sectional shape, rather than biochemical processes, would be the factor altering the mechanics of the unit surface of the wall (see Supplemental Fig. S2, G and H, of Amsbury et al., 2016). The irregular cell shape as viewed in the cross-section and inner wall thickness may explain the anomaly in stomatal opening, which requires further investigation through FE modeling. It should be noted that an earlier study on the chemical alteration of the guard cell wall during development in *Funaria hygrometrica* by Merced and Renzaglia (2014) reserves a special role for rhamnogalacturonan I distribution in guard cell walls, in addition to the role of homogalacturonan. Further assessment of the potential contribution of other types of pectin in guard cell mechanics may provide answers to some of the outstanding questions.

The Roles of Pectin-Induced Stiffening and Adjacent Subsidiary Cells in the Polar Prevention of Guard Cell Elongation and Stomatal Opening

Pectin biochemistry was also the focus of a modeling study that suggests deesterification of pectin at poles of

guard cells to underlie pore opening (Carter et al., 2017). Ventral walls of guard cells are generally thicker compared with dorsal walls (Meidner and Mansfield, 1968; Renzaglia et al., 2017). Using AFM stiffness measurements, Carter et al. (2017) suggested that ventral wall thickening does not occur in young guard cells, while the stomata are still as functional as in mature guard cells. This is consistent with predictions made by an FE model developed in the same article, similar to the model by Woolfenden et al. (2017), suggesting the effect of ventral wall thickening to be minimal in stomatal opening, as also proposed by Cooke et al. (1976). Interestingly, Carter et al. (2017) showed that pectin is unesterified in guard cell poles and that the application of polygalacturonases rendered guard cells incapable of opening the aperture. Probing the stiffness of the enzyme-treated guard cells with AFM, the authors suggested that the guard cells' dysfunction arises from the removal of polar stiffening due to polygalacturonase treatment. However, from the image provided, it seems that, rather than the removal of stiffness from poles, the enzyme treatment had caused the relative apparent stiffness to spread over a broader region of the guard cell walls (see Fig. 4I of Carter et al., 2017). Furthermore, it should be considered that the enzyme treatment also might change the turgor pressure in the guard cells or subsidiary cells. Neither of these possible collateral effects nor any possible changes in cell ultrastructure resulting from pectin modification were verified.

The simulations predicted that, whether or not the cells are fixed at the poles, a threshold pressure (1 MPa) is required to initiate aperture opening. A threshold pressure has indeed been observed in biological samples. This lag in response was found to be due to the antagonizing effect of turgid subsidiary cells (Franks and Farquhar, 1998). As the pressure in these cells approaches zero, for example due to damage, the threshold pressure vanishes and the pore opens at guard cell pressures close to zero. The role of subsidiary cells is not spelled out in the model by Carter et al. (2017), but the modeling equivalent of an external constraining obstacle was nevertheless incorporated, only motivated by an unrelated biological feature. Carter et al. (2017) used the experimental finding of the stiffened guard cell poles to hypothesize that polar stiffening augments the pore opening at a given turgor pressure. They argued that the stiffened polar cell wall fixes the cell ends in place, and this concept was implemented by adding a boundary condition to the Woolfenden et al. (2017) FE model, on which the model by Carter et al. (2017) is based. This boundary condition consisted of fixing the poles in place. The problem of this translation of a biological concept into the FE model is that, to replicate the polar stiffening due to pectin deesterification, it should have been implemented as a property (e.g. locally elevated Young's modulus) of the guard cell wall. Instead, the constrained displacement boundary condition removes displacement degrees of freedom at the poles, which biologically can only reflect an external constraint such as the above-mentioned

surrounding subsidiary cells. Therefore, while the simulations are consistent with the findings by Franks and Farquhar (1998), the biological justification used by Carter et al. (2017) to implement the boundary condition merits reassessing. It is important to note that, as mentioned before, the model developed by Cooke et al. (1976; videos are available under hdl.handle.net/1813/43793 and hdl.handle.net/1813/43794) did not demonstrate a considerable polar expansion even though the poles were free to displace. Clearly, the choice of the model geometry is a crucial step in model construction.

Future studies to address these questions, specifically the effects of cell cross-sectional shape and subsidiary cells on the stomatal complex, have the potential to further elucidate the functioning of pectin in stomatal mechanics. Suffice it to say that the scenarios proposed

OUTSTANDING QUESTIONS

- Transverse isotropy and restriction of lateral expansion are attributed mainly to cellulose microfibrils. Why then does depolymerization or disturbed actin functioning cause swelling in some cells although cellulose microfibrils may have remained seemingly intact?
- How does the mechanical stresses evolve in the cell wall during the cell growth?
- Is the reorganization of microtubules in cells located adjacent to a tissue injury or a perturbation a consequence of a change in the mechanical stress status or a response to a biological/chemical signal triggered due to loss of homeostasis?
- How can the softening proposed at the convex side of anticlinal walls in pavement cells be reconciled with the proposed stiffening suggested due to cellulose reinforcement at adjacent periclinal walls?
- What are the linking components between mechanical stress and strain in the wall and a biological response such as microtubule realignment? Do they function based on network tension or compression?
- Contradictory reports on the mechanics of guard cell deformation point at the necessity to judiciously assess the influence of parameters such as cell geometry, microfibril-mediated radial anisotropy, and pectin. Further, do guard cells employ different, and perhaps redundant, mechanical strategies to open the pore throughout their development?
- Are dumbbell-shaped guard cells in monocots mechanically similar to their kidney-shaped dicot counterparts?

by various groups, even if seemingly inconsistent, provide food for further thought. We wonder whether guard cells use different mechanisms redundantly, or distinctly at different stages of development. An observation reinforcing this hypothesis may be the change from semicircular to elliptical cross-section between early-stage and mature guard cells (Merced and Renzaglia, 2014).

REMARK

FE modeling is a powerful tool that has been employed successfully to simulate the behavior of geometrically complex plant cells. The modeling technique has been used to localize and predict stress and strain in cells with the purpose to understand the underlying biological mechanisms, and it has been applied to both reversible and irreversible processes, such as guard cell movement and cell growth events, respectively. Despite, or because, the rapid adoption of FE modeling by the plant cell community, care must be taken in interpreting FE results. FE modeling, as with any modeling strategy, is subject to a dependency on the quality of inputs; flawed inputs result in flawed outcomes. Oversimplification or misrepresentation of the model components, ranging from the geometry, material behavior, or boundary conditions, has the potential to bear misleading results or to reinforce a bias as a self-fulfilling prophecy (see Outstanding Questions). Good modeling practice is to experiment with and eliminate the parameters that may affect the outcome before accepting the remaining ones. It is the responsibility of the user to ascertain that the inputs agree well with the physics of the problem and that the output is biologically relevant, which requires a proper understanding of both the physics and the biology of the problem.

LITERATURE CITED

Amada G, Onoda Y, Ichie T, Kitayama K (2017) Influence of leaf trichomes on boundary layer conductance and gas-exchange characteristics in *Metrosideros polymorpha* (Myrtaceae). Biotropica **49:** 482–492

Amsbury S, Hunt L, Elhaddad N, Baillie A, Lundgren M, Verhertbruggen Y, Scheller HV, Knox JP, Fleming AJ, Gray JE (2016) Stomatal function requires pectin de-methyl-esterification of the guard cell wall. Curr Biol **26:** 2899–2906

Armour WJ, Barton DA, Law AM, Overall RL (2015) Differential growth in periclinal and anticlinal walls during lobe formation in *Arabidopsis* cotyledon pavement cells. Plant Cell **27:** 2484–2500

Aylor DE, Parlange JY, Krikorian AD (1973) Stomatal mechanics. Am J Bot **60:** 163–171

Bascom CS, Hepler PK, Bezanilla M (2018) Interplay between ions, the cytoskeleton, and cell wall properties during tip growth. Plant Physiol **176:** 28–40

Baskin TI (2005) Anisotropic expansion of the plant cell wall. Annu Rev Cell Dev Biol **21:** 203–222

Bassel GW, Stamm P, Mosca G, Barbier de Reuille P, Gibbs DJ, Winter R, Janka A, Holdsworth MJ, Smith RS (2014) Mechanical constraints imposed by 3D cellular geometry and arrangement modulate growth patterns in the *Arabidopsis* embryo. Proc Natl Acad Sci USA **111:** 8685–8690

Belteton S, Sawchuk MG, Donohoe BS, Scarpella E, Szymanski DB (2018) Reassessing the roles of PIN proteins and anticlinal microtubules during pavement cell morphogenesis. Plant Physiol **176:** 432–449

Bidhendi AJ, Geitmann A (2016) Relating the mechanics of the primary plant cell wall to morphogenesis. J Exp Bot **67:** 449–461

Bidhendi AJ, Korhonen RK (2012) A finite element study of micropipette aspiration of single cells: effect of compressibility. Comput Math Methods Med **2012:** 192618

Bolduc JE, Lewis LJ, Aubin CÉ, Geitmann A (2006) Finite-element analysis of geometrical factors in micro-indentation of pollen tubes. Biomech Model Mechanobiol **5:** 227–236

Boudaoud A (2010) An introduction to the mechanics of morphogenesis for plant biologists. Trends Plant Sci **15:** 353–360

Boudon F, Chopard J, Ali O, Gilles B, Hamant O, Boudaoud A, Traas J, Godin C (2015) A computational framework for 3D mechanical modeling of plant morphogenesis with cellular resolution. PLoS Comput Biol **11:** e1003950

Bozorg B, Krupinski P, Jönsson H (2014) Stress and strain provide positional and directional cues in development. PLoS Comput Biol **10:** e1003410

Braybrook SA, Peaucelle A (2013) Mechano-chemical aspects of organ formation in *Arabidopsis thaliana*: the relationship between auxin and pectin. PLoS ONE **8:** e57813

Campàs O, Mahadevan L (2009) Shape and dynamics of tip-growing cells. Curr Biol **19:** 2102–2107

Carter R, Woolfenden H, Baillie A, Amsbury S, Carroll S, Healicon E, Sovatzoglou S, Braybrook S, Gray JE, Hobbs J, et al (2017) Stomatal opening involves polar, not radial, stiffening of guard cells. Curr Biol **27:** 2974–2983

Cooke JR, De Baerdemaeker JG, Rand RH, Mang HA (1976) A finite element shell analysis of guard cell deformations. Trans ASAE **19:** 1107–1121

Cooke JR, Rand RH, Mang HA, De Baerdemaeker JG, Lee JY (2008) Shell analysis of elliptical guard cells in higher plants: a review. *In* JF Abel, JR Cooke, eds, International Conference on Computation of Shell and Spatial Structures. IASS-IACM 2008: "Spanning Nano to Mega," Cornell University, Ithaca, NY, USA, pp. 723–726

Cosgrove DJ (2016) Plant cell wall extensibility: connecting plant cell growth with cell wall structure, mechanics, and the action of wall-modifying enzymes. J Exp Bot **67:** 463–476

Cosgrove DJ (2018) Diffuse growth of plant cell walls. Plant Physiol **176:** 16–27

DeMichele DW, Sharpe PJ (1973) An analysis of the mechanics of guard cell motion. J Theor Biol **41:** 77–96

Dumais J (2013) Modes of deformation of walled cells. J Exp Bot **64:** 4681–4695

Dumais J, Shaw SL, Steele CR, Long SR, Ray PM (2006) An anisotropic-viscoplastic model of plant cell morphogenesis by tip growth. Int J Dev Biol **50:** 209–222

Dyson R, Jensen O (2010) A fibre-reinforced fluid model of anisotropic plant cell growth. J Fluid Mech **655:** 472–503

Edwards M, Meidner H, Sheriff D (1976) Direct measurements of turgor pressure potentials of guard cells. II. The mechanical advantage of subsidiary cells, the spannungsphase, and the optimum leaf water deficit. J Exp Bot **27:** 163–171

Elliott A, Shaw SL (2018) Update. Plant cortical microtubule arrays. Plant Physiol **176:** 94–105

Fayant P, Girlanda O, Chebli Y, Aubin CÉ, Villemure I, Geitmann A (2010) Finite element model of polar growth in pollen tubes. Plant Cell **22:** 25792593

Forouzesh E, Goel A, Mackenzie SA, Turner JA (2013) In vivo extraction of *Arabidopsis* cell turgor pressure using nanoindentation in conjunction with finite element modeling. Plant J **73:** 509–520

Forterre Y, Skotheim JM, Dumais J, Mahadevan L (2005) How the Venus fly trap snaps. Nature **433:** 421–425

Franks P, Farquhar G (1998) A study of stomatal mechanics using the cell pressure probe. Plant Cell Environ **21:** 94–100

Franks PJ, Farquhar GD (2007) The mechanical diversity of stomata and its significance in gas-exchange control. Plant Physiol **143:** 78–87

Fu Y, Gu Y, Zheng Z, Wasteneys G, Yang Z (2005) *Arabidopsis* interdigitating cell growth requires two antagonistic pathways with opposing action on cell morphogenesis. Cell **120:** 687–700

Gasser TC, Ogden RW, Holzapfel GA (2006) Hyperelastic modelling of arterial layers with distributed collagen fibre orientations. J R Soc Interface **3:** 15–35

Geitmann A (2016) Actuators acting without actin. Cell **166:** 15–17

Geitmann A, Hush J, Overall R (1997) Inhibition of ethylene biosynthesis does not block microtubule re-orientation in wounded pea roots. Protoplasma 198: 135–142

Geitmann A, Ortega JK (2009) Mechanics and modeling of plant cell growth. Trends Plant Sci 14: 467–478

Goriely A, Tabor M (2003) Self-similar tip growth in filamentary organisms. Phys Rev Lett 90: 108101

Green PB (1962) Mechanism for plant cellular morphogenesis. Science 138: 1404–1405

Hamant O, Heisler MG, Jönsson H, Krupinski P, Uyttewaal M, Bokov P, Corson F, Sahlin P, Boudaoud A, Meyerowitz EM, et al (2008) Developmental patterning by mechanical signals in Arabidopsis. Science 322: 1650–1655

Hofhuis H, Moulton D, Lessinnes T, Routier-Kierzkowska AL, Bomphrey RJ, Mosca G, Reinhardt H, Sarchet P, Gan X, Tsiantis M, et al (2016) Morphomechanical innovation drives explosive seed dispersal. Cell 166: 222–233

Huang R, Becker A, Jones I (2012) Modelling cell wall growth using a fibre-reinforced hyperelastic-viscoplastic constitutive law. J Mech Phys Solids 60: 750–783

Huang R, Becker AA, Jones IA (2015) A finite strain fibre-reinforced viscoelasto-viscoplastic model of plant cell wall growth. J Eng Math 95: 121–154

Hwang JU, Gu Y, Lee YJ, Yang Z (2005) Oscillatory ROP GTPase activation leads the oscillatory polarized growth of pollen tubes. Mol Biol Cell 16: 5385–5399

Jacques E, Verbelen JP, Vissenberg K (2013) Mechanical stress in Arabidopsis leaves orients microtubules in a 'continuous' supracellular pattern. BMC Plant Biol 13: 163

Jacques E, Verbelen JP, Vissenberg K (2014) Review on shape formation in epidermal pavement cells of the Arabidopsis leaf. Funct Plant Biol 41: 914–921

Julkunen P, Kiviranta P, Wilson W, Jurvelin JS, Korhonen RK (2007) Characterization of articular cartilage by combining microscopic analysis with a fibril-reinforced finite-element model. J Biomech 40: 1862–1870

Kha H, Tuble SC, Kalyanasundaram S, Williamson RE (2010) WallGen, software to construct layered cellulose-hemicellulose networks and predict their small deformation mechanics. Plant Physiol 152: 774–786

Klahre U, Becker C, Schmitt AC, Kost B (2006) Nt-RhoGDI2 regulates Rac/Rop signaling and polar cell growth in tobacco pollen tubes. Plant J 46: 1018–1031

Korn RW (1976) Concerning the sinuous shape of leaf epidermal cells. New Phytol 77: 153–161

Kost B (2008) Spatial control of Rho (Rac-Rop) signaling in tip-growing plant cells. Trends Cell Biol 18: 119–127

Kost B, Lemichez E, Spielhofer P, Hong Y, Tolias K, Carpenter C, Chua NH (1999) Rac homologues and compartmentalized phosphatidylinositol 4,5-bisphosphate act in a common pathway to regulate polar pollen tube growth. J Cell Biol 145: 317–330

Kotchoni SO, Zakharova T, Mallery EL, Le J, El-Assal Sel-D, Szymanski DB (2009) The association of the Arabidopsis actin-related protein2/3 complex with cell membranes is linked to its assembly status but not its activation. Plant Physiol 151: 2095–2109

Kroeger J, Geitmann A (2011) Modeling pollen tube growth: feeling the pressure to deliver testifiable predictions. Plant Signal Behav 6: 1828–1830

Kroeger JH, Geitmann A (2012) Pollen tube growth: getting a grip on cell biology through modeling. Mech Res Commun 42: 32–39

Kroeger JH, Geitmann A, Grant M (2008) Model for calcium dependent oscillatory growth in pollen tubes. J Theor Biol 253: 363–374

Lee JY (1986) A finite element for shell analysis and its application to biological objects. PhD thesis. Cornell University, Ithaca, NY

Lin D, Cao L, Zhou Z, Zhu L, Ehrhardt D, Yang Z, Fu Y (2013) Rho GTPase signaling activates microtubule severing to promote microtubule ordering in Arabidopsis. Curr Biol 23: 290–297

Majda M, Grones P, Sintorn IM, Vain T, Milani P, Krupinski P, Zagórska-Marek B, Viotti C, Jönsson H, Mellerowicz EJ, et al (2017) Mechanochemical polarization of contiguous cell walls shapes plant pavement cells. Dev Cell 43: 290–304

Mathur J (2004) Cell shape development in plants. Trends Plant Sci 9: 583–590

Mathur J, Spielhofer P, Kost B, Chua N (1999) The actin cytoskeleton is required to elaborate and maintain spatial patterning during trichome cell morphogenesis in Arabidopsis thaliana. Development 126: 5559–5568

Meidner H, Mansfield TA (1968) Physiology of Stomata. Tata McGraw-Hill, Bombay

Merced A, Renzaglia K (2014) Developmental changes in guard cell wall structure and pectin composition in the moss Funaria: implications for function and evolution of stomata. Ann Bot 114: 1001–1010

Niklas KJ (1992) Plant biomechanics: an engineering approach to plant form and function. PhD thesis. University of Chicago, Chicago

Oelschlägel B, Gorb S, Wanke S, Neinhuis C (2009) Structure and biomechanics of trapping flower trichomes and their role in the pollination biology of Aristolochia plants (Aristolochiaceae). New Phytol 184: 988–1002

Palin R, Geitmann A (2012) The role of pectin in plant morphogenesis. Biosystems 109: 397–402

Panteris E, Galatis B (2005) The morphogenesis of lobed plant cells in the mesophyll and epidermis: organization and distinct roles of cortical microtubules and actin filaments. New Phytol 167: 721–732

Parre E, Geitmann A (2005) Pectin and the role of the physical properties of the cell wall in pollen tube growth of Solanum chacoense. Planta 220: 582–592

Peaucelle A, Braybrook SA, Le Guillou L, Bron E, Kuhlemeier C, Höfte H (2011) Pectin-induced changes in cell wall mechanics underlie organ initiation in Arabidopsis. Curr Biol 21: 1720–1726

Raschke K (1975) Stomatal action. Annu Rev Plant Physiol 26: 309–340

Raven JA (2014) Speedy small stomata? J Exp Bot 65: 1415–1424

Renzaglia KS, Villarreal JC, Piatkowski BT, Lucas JR, Merced A (2017) Hornwort stomata: architecture and fate shared with 400 million year old fossil plants without leaves. Plant Physiol 174: 788–797

Roelfsema MRG, Hedrich R (2005) In the light of stomatal opening: new insights into 'the Watergate'. New Phytol 167: 665–691

Rojas ER, Hotton S, Dumais J (2011) Chemically mediated mechanical expansion of the pollen tube cell wall. Biophys J 101: 1844–1853

Rui Y, Anderson CT (2016) Functional analysis of cellulose and xyloglucan in the walls of stomatal guard cells of Arabidopsis. Plant Physiol 170: 1398–1419

Sampathkumar A, Krupinski P, Wightman R, Milani P, Berquand A, Boudaoud A, Hamant O, Jönsson H, Meyerowitz EM (2014) Subcellular and supracellular mechanical stress prescribes cytoskeleton behavior in Arabidopsis cotyledon pavement cells. eLife 3: e01967

Sanati Nezhad A, Geitmann A (2015) Tip growth in walled cells: cellular expansion and invasion mechanisms. In C Cuerrier, A Pelling, eds, Cells, Forces and the Microenvironment. Pan Stanford Publishing, pp 335–356

Sanati Nezhad A, Naghavi M, Packirisamy M, Bhat R, Geitmann A (2013) Quantification of the Young's modulus of the primary plant cell wall using Bending-Lab-On-Chip (BLOC). Lab Chip 13: 2599–2608

Sharpe PJ, Wu HI (1978) Stomatal mechanics: volume changes during opening. Plant Cell Environ 1: 259–268

Sun EQ (2006) Shear locking and hourglassing in MSC Nastran, ABAQUS, and ANSYS. In MSC Software Corporation's 2006 Americas Virtual Product Development Conference: Evolution to Enterprise Simulation. MSC Software, Santa Ana, CA, presentation 27, pp. 1–9

Szymanski DB, Marks MD, Wick SM (1999) Organized F-actin is essential for normal trichome morphogenesis in Arabidopsis. Plant Cell 11: 2331–2347

Szymanski DB, Staiger CJ (2018) The actin cytoskeleton: functional arrays for cytoplasmic organization and cell shape control. Plant Physiol 176: 106–118

Tissier A (2012) Glandular trichomes: what comes after expressed sequence tags? Plant J 70: 51–68

Torode TA, O'Neill RE, Marcus SE, Cornuault V, Pose-Albacete S, Lauder RP, Kracun SK, Gro Rydahl M, Andersen MCF, Willats WGT, et al (2018) Branched pectic galactan in phloem-sieve-element cell walls: implications for cell mechanics. Plant Physiol (in press) https://doi.org/10.1104/pp.17.01568

Von Mohl H (1856) Welche Ursachen bewirken die Erweiterung und Verengung der Spaltöffnungen. Bot Z 14: 697–704

Williamson RE (1990) Alignment of cortical microtubules by anisotropic wall stresses. Funct Plant Biol 17: 601–613

Woolfenden HC, Bourdais G, Kopischke M, Miedes E, Molina A, Robatzek S, Morris RJ (2017) A computational approach for inferring the cell wall properties that govern guard cell dynamics. Plant J 92: 5–18

Xu T, Wen M, Nagawa S, Fu Y, Chen JG, Wu MJ, Perrot-Rechenmann C, Friml J, Jones AM, Yang Z (2010) Cell surface- and rho GTPase-based auxin signaling controls cellular interdigitation in Arabidopsis. Cell 143: 99–110

Yanagisawa M, Desyatova AS, Belteton SA, Mallery EL, Turner JA, Szymanski DB (2015) Patterning mechanisms of cytoskeletal and cell wall systems during leaf trichome morphogenesis. Nat Plants **1:** 15014

Yi H, Puri VM (2012) Architecture-based multiscale computational modeling of plant cell wall mechanics to examine the hydrogen-bonding hypothesis of the cell wall network structure model. Plant Physiol **160:** 1281–1292

Zerzour R, Kroeger J, Geitmann A (2009) Polar growth in pollen tubes is associated with spatially confined dynamic changes in cell mechanical properties. Dev Biol **334:** 437–446

Zhang C, Halsey LE, Szymanski DB (2011) The development and geometry of shape change in *Arabidopsis thaliana* cotyledon pavement cells. BMC Plant Biol **11:** 27

Ziegenspeck A (1955) Das Vorkommen von Fila in radialer Anordnung in den Schliesszellen. Protoplasma **44:** 385–388